The longitudinal electrical conductivity of metal-matrix composites at cryogenic temperature in the presence of a longitudinal magnetic field

Part 1 *Solution of the linearized Boltzmann equation*

FRANCESC S. ROIG
College of Creative Studies, University of California, Santa Barbara, California 93106, USA
JACQUES E. SCHOUTENS*
MMCIAC, Kaman Tempo, 816 State Street, Santa Barbara, California 93102, USA

We solve the Boltzmann equation in the relaxation time approximation with parallel ***E*** and ***B*** fields parallel to the continuous fibres reinforcing a metal matrix. It is shown that this solution is identical to that described by us elsewhere, except for the addition of the cyclotron frequency. The addition of the cyclotron frequency term shows that the electrons follow helical paths as they drift down the composite. The boundary considered is either the external or the internal surface of a cylinder representing the fibre. To apply this solution to metal-matrix composite materials we assumed that the cylindrical fibres are non-conducting cylinders in a matrix of pure crystalline metal. The electron mean free path is never greater than half the fibre separation distance. In a companion paper we discuss the application of this solution to metal-matrix composites.

1. Introduction

With the exception of our work reported elsewhere [1], no theoretical analyses have been found which predict correctly the electrical conductivity of continuous-fibre reinforced metal-matrix composites (MMC) at cryogenic temperatures. As the temperature decreases from room temperature, the composite resistivity is expected to decrease steadily until at cryogenic temperatures, it will rise sharply by orders of magnitude. The steady decrease in resistivity is due to thermal effects in the matrix metal [2]. The sharp increase in resistivity at cryogenic temperature has been referred to by Dingle [3] and others [4–6] as the "size effect". This effect is caused by the electron transport for temperature conditions in which the electron scattering mean free path is of the order of, or greater than, the spacing between fibres. The electron scattering is produced by the fibre surfaces and, on a macroscopic scale, manifests itself as a greatly increased resistance [1]. Thus, the fibres act as scattering boundaries, thereby modifying considerably the electron conduction of the composite. In these kinds of analyses the resistivity of the fibres is generally considered to be orders of magnitude greater than that of the matrix metal. Therefore, the electrical conductivity of MMC materials is generally dominated by the matrix conductivity.

Although there are a number of macroscopic conductivity models to predict the electrical conductivity of MMC, no microscopic models, particularly those dealing with the electron behaviour at low temperatures, could be found [7], except for the work already cited [1]. There are no conductivity (or resistivity) data at cryogenic temperatures. Macroscopic models are of two kinds: conduction along the fibre and conduction transverse to the fibre direction. The first kind is based upon some variation of the Rule of Mixtures, assuming the matrix conduction to be dominant. The transverse electrical conductivity models exhibit various degrees of complexity [8–11] including concepts of percolation [12–14]. Both kinds of model do not predict correctly the electrical conductivity or resistivity of MMC at room temperature and below, and fail altogether below nitrogen temperature. A model developed by Schoutens and Roig [15] correctly predicts the transverse electrical resistivity of MMC above liquid nitrogen temperatures.

A number of experimental studies on the electrical conductivity of metal matrix and *in situ* composite materials have been reported [16–21]. In these studies, experimental results are discussed and related to conduction models. These models are either modified forms of the Rule of Mixtures or simple equations based on Dingle's asymptotic solution for electrical conduction in thin wires [3], and thin films, when the reinforcing filaments are either much larger or much

*To whom correspondence should be addressed.

0022–2461/87 $03.00 + .12

smaller than the bulk electron mean free path. To some extent, these models provide a simple theoretical explanation of the observed phenomena, but because of their simplicity, often fail to provide a satisfactory insight into the phenomena of low-temperature resistivity in these composites. Moreover, these models are limited to the experiments under discussion and, consequently, are inadequate for the prediction of the electrical behaviour of composites at low temperatures.

As mentioned above, the theory of Roig and Schoutens [1] is founded on a solution of the linearized Boltzmann equation with an electric field in the direction of the fibres. The case for the electric field normal to the fibre direction presents considerable theoretical difficulties, due mainly to the geometry involved [22]. The Boltzmann equation and its solutions were also applied to describe the resistivity phenomena of thin reaction regions and thin-walled tubes around a non-conducting fibre [23]. In these developments, the Boltzmann equation and its solutions are central to an understanding of low-temperature electrical conduction phenomena in metal matrix and *in situ* composites. Solutions to the Boltzmann equation are needed to describe electron and phonon scattering and transport phenomena in the matrix as a result of their interaction with fibre surfaces [24].

This paper is the first of two papers dealing with the effects of magnetic fields upon the electrical conductivity of continuous-fibre reinforced metals. This paper deals with the solution of the linearized Boltzmann equation, and the companion paper deals with its application to composite materials [29].

In the present paper, the magnetic field vector is assumed to be parallel to the fibres and the electric field vector is also parallel to the fibres. The approach used is to solve the linearized Boltzmann equation in the presence of these fields. The mean free path for internal scattering in the metal matrix is assumed to be no greater than half the fibre separation and, consequently, problems associated with overlapping scattering regions around each fibre are neglected. In the solution discussed in this paper, we apply the boundary conditions for scattering from the external surface of a cylinder and obtain the solution in the region outside the fibre when the fibres are non-conducting. If the boundary condition is applied to the internal surface of the cylinder, we obtain the solution for the case of a conducting fibre in a non-conducting matrix. For either case, the solution exhibits cylindrical symmetry. A physical interpretation of the solution is made: the electric field alone produces the drift current, and the longitudinal magnetic field modifies the electron trajectories from straight lines to circular helical paths, with the helical axis parallel to the fibres, as asserted by Chambers [5]. We point out that the solution of the Boltzmann equation for a thin wire in a magnetic field parallel to the wire obtained by Dingle [3] but was never published.

In the second and companion paper, we integrate the solution of the Boltzmann equation, discussed in this paper, and thereby obtain an integral expression for the conductivity with the stated fields.

2. The solution of the Boltzmann equation with cylindrical symmetry and longitudinal *E* and *B* fields

The linearized Boltzmann equation in rectangular coordinates, in the relaxation-time approximation, with applied $\boldsymbol{E}$ and $\boldsymbol{B}$ fields is [25]

$$\boldsymbol{v} \cdot \nabla_r F^1(\boldsymbol{r}, \boldsymbol{v}) + \frac{1}{\tau} F^1(\boldsymbol{r}, \boldsymbol{v}) - \frac{e}{m^*} (\boldsymbol{v} \times \boldsymbol{B}) \cdot \nabla_v F^1(\boldsymbol{r}, \boldsymbol{v}) = \frac{e}{m^*} \boldsymbol{E} \cdot \nabla_v F^0(v) \tag{1}$$

where $\boldsymbol{E}$ is the applied small electric field, e is the absolute value of the electronic charge and m^* is its effective mass, τ is the relaxation time, and F^1 is the change in the equilibrium distribution function F^0 when a small electric field is applied.

If we consider a unidirectional-fibre reinforced metal with the electric field $\boldsymbol{E}$ directed along the axis of the fibres and the $\boldsymbol{B}$ field pointing to the *opposite* direction to $\boldsymbol{E}$, Equation 1 becomes

$$v_x \frac{\partial F^1}{\partial x} + v_y \frac{\partial F^1}{\partial y} + \frac{F^1}{\tau} + \frac{e}{m^*} B \left\{ v_y \frac{\partial F^1}{\partial v_x} - v_x \frac{\partial F^1}{\partial v_y} \right\} = \frac{e}{m^*} E \frac{\partial F^0}{\partial v_z} \tag{2}$$

where the z axis is in the same direction as the electric field. We take the cylindrical coordinates $x = r \cos \varphi$, $y = r \sin \varphi$, $z = z$. Now, when the problem has cylindrical symmetry, F^1 does not depend on the angle φ and the partial derivatives appearing in Equation 2 are expressed as

$$\begin{aligned}
\frac{\partial}{\partial x} &= \cos \varphi \frac{\partial}{\partial r} - \frac{\sin \varphi}{r} \left(v_\varphi \frac{\partial}{\partial v_r} - v_r \frac{\partial}{\partial v_\varphi} \right) \\
\frac{\partial}{\partial y} &= \sin \varphi \frac{\partial}{\partial r} + \frac{\cos \varphi}{r} \left(v_\varphi \frac{\partial}{\partial v_r} - v_r \frac{\partial}{\partial v_\varphi} \right) \\
\frac{\partial}{\partial v_x} &= \cos \varphi \frac{\partial}{\partial v_r} - \sin \varphi \frac{\partial}{\partial v_\varphi} \\
\frac{\partial}{\partial v_y} &= \sin \varphi \frac{\partial}{\partial v_r} + \cos \varphi \frac{\partial}{\partial v_\varphi} \\
\frac{\partial}{\partial v_z} &= \frac{\partial}{\partial v_z}.
\end{aligned}$$

Consequently Equation 2 becomes

$$v_r \frac{\partial F^1}{\partial r} + v_\varphi \left(\frac{v_\varphi}{r} + \omega_0 \right) \frac{\partial F^1}{\partial v_r} - v_r \left(\frac{v_\varphi}{r} + \omega_0 \right) \frac{\partial F^1}{\partial v_\varphi} + \frac{F^1}{\tau} = \frac{eE}{m^*} \frac{\partial F^0(v)}{\partial v_z} \tag{3}$$

where $\omega_0 = eB/m^*$ is the cyclotron frequency of the electrons in the magnetic field. If $\omega_0 = 0$ (no magnetic field) Equation 3 reduces to the equation already solved and reported elsewhere [24]. If the $\boldsymbol{B}$ field is in the same direction as the $\boldsymbol{E}$ field, then just change ω_0 to $-\omega_0$ in Equation 3. Equation 3 can be integrated directly by using general methods for solving quasilinear partial differential equations [26]. The characteristic system of equations associated with Equation 3 is

$$\frac{\mathrm{d}r}{v_r} = \frac{\mathrm{d}v_r}{v_\varphi\,[(v_\varphi/r) + \omega_0]} = \frac{-\mathrm{d}v_\varphi}{v_r\,[(v_\varphi/r) + \omega_0]} = \frac{\mathrm{d}F^1}{A - (F^1/\tau)} \quad (4)$$

where

$$A = \frac{eE}{m^*}\frac{\partial F^0(v)}{\partial v_z} = \frac{eE}{m^*}\frac{v_z}{v}\frac{\partial F^0(v)}{\partial v} \quad (5)$$

$$v = (v_r^2 + v_\varphi^2 + v_z^2)^{1/2} \quad (6)$$

From

$$\frac{\mathrm{d}v_r}{v_\varphi\,[(v_\varphi/r) + \omega_0]} = -\frac{\mathrm{d}v_\varphi}{v_r\,[(v_\varphi/r) + \omega_0]}$$

it follows immediately that

$$v_r^2 + v_\varphi^2 = \text{constant} \equiv C_1^2 \quad (7)$$

and from

$$\frac{\mathrm{d}r}{v_r} = -\frac{\mathrm{d}v_\varphi}{v_r\,[(v_\varphi/r) + \omega_0]}$$

it follows that

$$rv_\varphi + \tfrac{1}{2}\omega_0 r^2 = \text{constant} \equiv C_2 \quad (8)$$

Next, we consider the following

$$\frac{\mathrm{d}r}{v_r} = \frac{\mathrm{d}F^1}{A - (F^1/\tau)} \quad (9)$$

Combining Equations 7 and 8 we can express v_r in terms of r and then Equation 9 becomes

$$\frac{r\,\mathrm{d}r}{[r^2C_1^2 - (C_2 - \frac{1}{2}\omega_0 r^2)^2]^{1/2}} = \frac{\mathrm{d}F^1}{A - (F^1/\tau)} \quad (10)$$

with

$$A = A\,[v_z, (v_r^2 + v_\varphi^2 + v_z^2)^{1/2}] = A\,[v_z, (C_1^2 + v_z^2)^{1/2}]$$

and v_z plays the role of a parameter in the integration of Equation 10. Letting $r^2/2 = w$ and integrating both sides of Equation 10 we obtain

$$\frac{1}{\omega_0}\sin^{-1}\left[\frac{-\omega_0^2 w + C_1^2 + \omega_0 C_2}{C_1(C_1^2 + 2\omega_0 C_2)^{1/2}}\right] = -\tau\ln\left(A - \frac{F^1}{\tau}\right) + \text{constant}$$

or, after replacing C_1 and C_2 by Equation 7 and 8, respectively, we arrive at

$$\left(A - \frac{F^1}{\tau}\right)\exp\left[\frac{1}{\omega_0\tau}\sin^{-1}\left(\frac{v_r^2 + v_\varphi^2 + \omega_0 rv_\varphi}{[(v_r^2 + v_\varphi^2)(v_r^2 + v_\varphi^2 + 2\omega_0 rv_\varphi + \omega_0^2r^2)]^{1/2}}\right)\right] = \text{constant} \equiv C_3 \quad (11)$$

The general solution of Equation 3 is obtained by setting an arbitrary relationship between C_1, C_2 and C_3: $C_3 = A[v_z, (C_1^2 + v_z^2)^{1/2}]f(C_1^2, C_2)$ where f is an arbitrary function. Therefore, in terms of the velocity and position of the electron we can write

$$\left(A - \frac{F^1}{\tau}\right)\exp\left[\frac{1}{\omega_0\tau}\sin^{-1}\left(\frac{v_r^2 + v_\varphi^2 + \omega_0 rv_\varphi}{[(v_r^2 + v_\varphi^2)(v_r^2 + v_\varphi^2 + 2\omega_0 rv_\varphi + \omega_0^2r^2)]^{1/2}}\right)\right] = A\,f\,(v_r^2 + v_\varphi^2, rv_\varphi + \tfrac{1}{2}\omega_0 r^2)$$

Finally, the general solution of the Boltzmann Equation 3 is

$$F^1 = \frac{eE\tau}{m^*}\frac{v_z}{v}\frac{\partial F^0(v)}{\partial v}\left\{1 - f(v_r^2 + v_\varphi^2, rv_\varphi + \tfrac{1}{2}\omega_0 r^2) \times \exp\left[-\frac{1}{\omega_0\tau}\sin^{-1}\left(\frac{v_r^2 + v_\varphi^2 + \omega_0 rv_\varphi}{[(v_r^2 + v_\varphi^2)(v_r^2 + v_\varphi^2 + 2\omega_0 rv_\varphi + \omega_0^2r^2)]^{1/2}}\right)\right]\right\} \quad (12)$$

The general solution Equation 12 can be rewritten in an alternative form more suitable for applying the boundary condition. We use the identity $\sin^{-1}x = (\pi/2) - \sin^{-1}[(1 - x^2)^{1/2}]$ and in Equation 12 we then have

$$f\exp\left(-\frac{1}{\omega_0\tau}\sin^{-1}x\right) = f\exp\left(-\frac{1}{\omega_0\tau}\left\{\frac{\pi}{2} - \sin^{-1}[(1 - x^2)^{1/2}]\right\}\right)$$

with

$$x = \frac{v_r^2 + v_\varphi^2 + \omega_0 rv_\varphi}{[(v_r^2 + v_\varphi^2)(v_r^2 + v_\varphi^2 + 2\omega_0 rv_\varphi + \omega_0^2r^2)]^{1/2}}$$

and absorbing the term $\exp(-\pi/2\omega_0\tau)$ into f so that there results the alternative form of the general solution, Equation 12:

$$F^1 = \frac{eE\tau}{m^*}\frac{v_z}{v}\frac{\partial F^0(v)}{\partial v}\left\{1 - f(v_r^2 + v_\varphi^2, rv_\varphi + \tfrac{1}{2}\omega_0 r^2) \times \exp\left[-\frac{1}{\omega_0\tau}\sin^{-1}\left(\frac{\omega_0 rv_r}{[(v_r^2 + v_\varphi^2)(v_r^2 + v_\varphi^2 + 2\omega_0 rv_\varphi + \omega_0^2r^2)]^{1/2}}\right)\right]\right\} \quad (13)$$

It is readily seen that the general solution, Equation 13, reduces to the general solution discussed elsewhere [24] when the term $\omega_0 \equiv 0$ ($B = 0$).

3. Construction of solutions satisfying the boundary conditions

We will now construct the solution in the region outside a cylinder of radius, a, when the scattering is completely diffusive ($p = 0$ in [1]). (A detailed discussion has recently appeared [27] on the specular probability distribution function which applies to surface-contaminated thin films.) This means that immediately after emerging from the surface, the electrons have directions distributed at random, that is $F^1(+|v_r|, v_\varphi, r = a) = 0$ or from Equation 13

$$1 - f(v_r^2 + v_\varphi^2,\ av_\varphi + \tfrac{1}{2}\omega_0 a^2)\exp\left[-\frac{1}{\omega_0\tau}\sin^{-1}\left(\frac{\omega_0 a|v_r|}{[(v_r^2 + v_\varphi^2)(v_r^2 + v_\varphi^2 + 2\omega_0 a v_\varphi + \omega_0^2 a^2)]^{1/2}}\right)\right] = 0 \tag{14}$$

Therefore, we need to find a function $f(u, s)$ such that

$$f(u, s)|_{r=a} = \exp\left[\frac{1}{\omega_0\tau}\sin^{-1}\left(\frac{\omega_0 a|v_r|}{D(a)}\right)\right]$$

with $u = v_r^2 + v_\varphi^2$ and $s = rv_\varphi + (\omega_0 r^2/2)$, where

$$D(r) = [(v_r^2 + v_\varphi^2)(v_r^2 + v_\varphi^2 + 2\omega_0 r v_\varphi + \omega_0^2 r^2)]^{1/2}$$

Since

$$a|v_r| = [a^2 u - (s - \tfrac{1}{2}\omega_0 a^2)^2]^{1/2}|_{r=a}$$

we have for this function

$$f(u, s) = \exp\left[\frac{1}{\omega_0\tau}\sin^{-1}\left(\frac{\omega_0[a^2 u - (s - \frac{1}{2}\omega_0 a^2)^2]^{1/2}}{[u(u + 2\omega_0 s)]^{1/2}}\right)\right]$$

and the boundary condition, Equation 14, is satisfied.

Finally, the solution for the region outside the cylinder is

$$F^1 = \tau A\,[1 - \exp(-\psi/\omega_0\tau)] \tag{15}$$

where $\psi = \alpha - \delta$, where $r \geqslant a$, and where a is the fibre radius, $\alpha = \sin^{-1}[\omega_0 r v_r/D(r)]$ and

$$\delta = \sin^{-1}\left(\frac{\omega_0}{D(r)}\{a^2(v_r^2 + v_\varphi^2) - [rv_\varphi + \tfrac{1}{2}\omega_0(r^2 - a^2)]^2\}^{1/2}\right)$$

For the region inside the cylinder the boundary condition is $F^1(-|v_r|, v_\varphi, r = a) = 0$ and proceeding as before we obtain the same expression as Equation 15 for the solution, except that $\psi = \alpha + \delta$ where $r \leqslant a$. This is Dingle's result [3].

4. Geometrical interpretation of the solution

In this section we discuss the interpretation of the solution of the Boltzmann equation in terms of the electron trajectories in the presence of cylindrical boundaries.

When there is an electric field without a magnetic field, the solution of the Boltzmann equation involves only rectilinear trajectories for the electrons. When a magnetic field, which can be parallel or antiparallel to the electric field, is added to the electric field, the trajectories are no longer linear but can be considered to be helical paths, that is, the electrons spiral along the direction of the magnetic field. Such a path is shown in Fig. 1.

If $\boldsymbol{v}$ is the electron velocity at a given point in the metal, then we want to verify that the solution to the Boltzmann equation with a longitudinal magnetic field can be written as

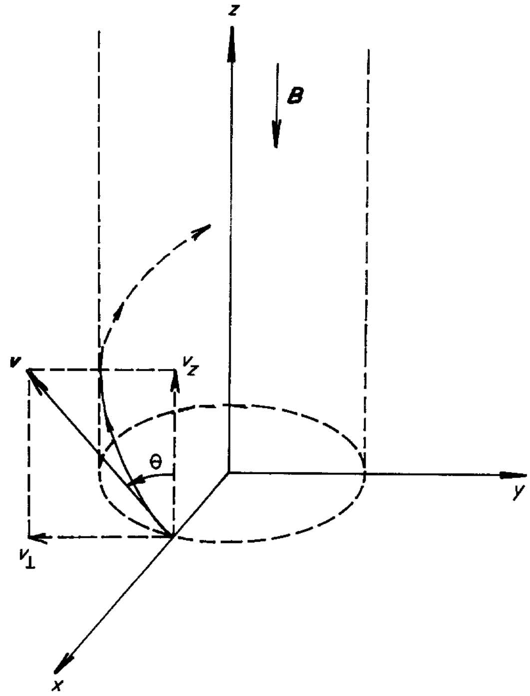

Figure 1 Coordinates and nomenclature for helical paths of electrons.

$$F^1 = A\,(1 - e^{-s/v\tau}) \tag{16}$$

where s is the length along the helical path obtained proceeding backward from the direction of $\boldsymbol{v}$ to the scattering boundary. The radius of the helical path is r_0 and is given by $r_0 = (v/\omega_0)\sin\theta$ where θ is the angle that $\boldsymbol{v}$ makes with the z axis. The projection of $\boldsymbol{v}$ on the x–y plane is given by $v_\perp = v\sin\theta = (v_r^2 + v_\varphi^2)^{1/2}$. We can write $s/v\tau = r_0\psi/v_\perp\tau$, but $r_0/v_\perp = 1/\omega_0$ so that $s/v\tau = \psi/\omega_0\tau$ where ψ is the angle described in the x–y plane by the projection of the helical path on this plane.

Next, we derive the angle ψ using geometric arguments. As shown in Fig. 2, the circular arc PB described by the electron in the x–y plane defines the angle ψ. We have $\beta = (\pi/2) + \phi$ and $r_c^2 = r^2 + r_0^2 + 2rr_0\sin\phi$ and also $\cos\gamma = (r^2 + r_c^2 - r_0^2)/2rr_c$ so that we have

$$\cos\gamma = \frac{r + r_0\sin\phi}{[r^2 + r_c^2 + 2rr_0\sin\phi]^{1/2}} \tag{17}$$

Now $\alpha = \pi - \gamma - \beta$, $\psi = \alpha - \delta$ or $\psi = (\pi/2) - \gamma - \phi - \delta$. Moreover $\cos\delta = (r_c^2 + r_0^2 - a^2)/2r_0 r_c$. Therefore, we obtain

$$\cos\delta = \frac{r^2 + 2r_0^2 - a^2 + 2rr_0\sin\phi}{2r_0\,[r^2 + r_0^2 + 2rr_0\sin\phi]^{1/2}} \tag{18}$$

so that ψ becomes

$$\psi = \frac{\pi}{2} - \phi - \cos^{-1}\left[\frac{r + r_0\sin\phi}{(r^2 + r_0^2 + 2rr_0\sin\phi)^{1/2}}\right] - \cos^{-1}\left[\frac{r^2 + 2r_0^2 - a^2 + 2rr_0\sin\phi}{2r_0\,(r^2 + r_0^2 + 2rr_0\sin\phi)^{1/2}}\right] \tag{19}$$

Next, we use $\sin\phi = v_\varphi/(v_r^2 + v_\varphi^2)^{1/2}$ and the identity $\sin^{-1}x = (\pi/2) - \cos^{-1}x$, so that Equation 19

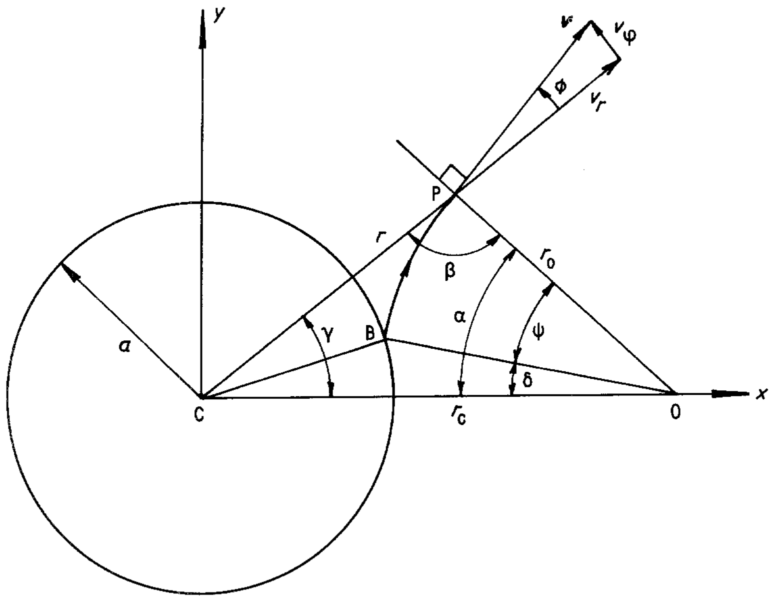

Figure 2 Coordinates and angles for a portion of the helical path projected onto the x–y plane.

becomes, after some algebra,

$$\psi = -\phi - \cos^{-1}\left[\frac{\omega_0 r + v_\varphi}{(v_r^2 + v_\varphi^2 + 2\omega_0 r v_\varphi + \omega_0^2 r^2)^{1/2}}\right] + \sin^{-1}\left\{\frac{v_r^2 + v_\varphi^2 + \omega_0 r v_\varphi + \frac{1}{2}\omega_0(r^2 - a^2)}{[(v_r^2 + v_\varphi^2)(v_r^2 + v_\varphi^2 + 2\omega_0 r v_\varphi + \omega_0^2 r^2)]^{1/2}}\right\} \quad (20)$$

In cylindrical coordinates the angle γ is given by

$$\gamma = \cos^{-1}\left[\frac{\omega_0 r + v_r}{(v_r^2 + v_\varphi^2 + 2\omega_0 r v_\varphi + \omega_0^2 r^2)^{1/2}}\right]$$

or

$$\gamma = \sin^{-1}\left[\frac{v_r}{(v_r^2 + v_\varphi^2 + 2\omega_0 r v_\varphi + \omega_0^2 r^2)^{1/2}}\right] \quad (21)$$

We can also take the arcsine of $\sin\phi = v_\varphi/(v_r^2 + v_\varphi^2)^{1/2}$ and apply to the sum $\gamma + \phi$ the identity [28],

$$\sin^{-1}x + \sin^{-1}y = \cos^{-1}[(1 - x^2)^{1/2}(1 - y^2)^{1/2} - xy] \quad (22)$$

for $x \geqslant 0$ and $y \geqslant 0$. Therefore

$$\gamma + \phi = \cos^{-1}\left\{\frac{\omega_0 r v_r}{[(v_r^2 + v_\varphi^2)(v_r^2 + v_\varphi^2 + 2\omega_0 r v_\varphi + \omega_0^2 r^2)]^{1/2}}\right\}$$

so that Equation 20 finally becomes

$$\psi = -\cos^{-1}\left\{\frac{\omega_0 r v_r}{[(v_r^2 + v_\varphi^2)(v_r^2 + v_\varphi^2 + 2\omega_0 r v_\varphi + \omega_0^2 r^2)]^{1/2}}\right\} + \sin^{-1}\left\{\frac{v_r^2 + v_\varphi^2 + \omega_0 r v_\varrho + \frac{1}{2}\omega_0^2(r^2 - a^2)}{[(v_r^2 + v_\varphi^2)(v_r^2 + v_\varphi^2 + 2\omega_0 r v_\varphi + \omega_0^2 r^2)]^{1/2}}\right\} \quad (23)$$

Next, we apply the identity $\cos^{-1}x = (\pi/2) - \sin^{-1}x$ to each term in Equation 23 and then use $\cos^{-1}x = \sin^{-1}[(1 - x^2)^{1/2}]$ so that we finally arrive at the result $\psi = \alpha - \delta$ where α and δ, shown in Fig. 2, are given precisely by the equations for α and δ, respectively, shown following Equation 15.

This concludes the proof of the geometric interpretation of the solution to the Boltzmann equation given at the beginning of this section.

For points inside the cylinder an entirely analogous geometrical construction would have given the result $\psi = \alpha + \delta$.

5. Conclusion

The Boltzmann equation in the relaxation-time approximation and in the presence of a longitudinal magnetic field has been solved directly using cylindrical coordinates. The presence of a magnetic field, parallel or antiparallel to the direction of the reinforcing fibres, simply adds the angular frequency $\omega_0 = eB/m^*$ to two of the coefficients in the Boltzmann Equation 3. This addition has the effect of causing the solution to be expressed in terms of helical trajectories for the electrons instead of straight-line trajectories, as in the case when the magnetic field is absent. This result follows from applying boundary conditions to the general solution of the Boltzmann equation. This boundary condition corresponds to the case of perfectly rough surfaces where the specular reflection parameter p is zero [1]. The boundary considered is either the external or the internal surface of a cylinder. This method of solution agrees with the geometrical method where the electron paths are considered to be helical.

To apply this solution to MMC material we assumed that the cylindrical fibres are non-conducting cylinders in a matrix of pure crystalline metal. The electron mean free path in the bulk metal is never greater than half the distance separating fibres. This assumption allows the fibres to be considered as independent scattering surfaces.

References

1. F. S. ROIG and J. E. SCHOUTENS, *J. Mater. Sci.* **21** (1986) 2409.
2. D. ABUKAY, K. V. RAO, S. ARAJS and Y. D. YAO, *Fiber Sci. Tech.* **10** (1977) 313.
3. R. B. DINGLE, *Proc. R. Soc.* **201A** (1949) 545.
4. E. H. SONDHEIMER, *Phys. Rev.* **80** (1950) 401.
5. R. G. CHAMBERS, *Proc. R. Soc.* **202A** (1950) 378.

6. D. K. C. MacDONALD and K. SARGINSON, *ibid.* **203A** (1951) 223.
7. S. ARAJS, personal communication (1985).
8. W. K. LIEBMANN and E. A. MILLER, *J. Appl. Phys.* **34** (1963) 2653.
9. J. W. RALEIGH, *Phil. Mag.* **34** (1892) 481.
10. L. K. H. van BECK, "Progress in Dielectrics", Vol. 7 (Heywood, London, 1967) p. 69.
11. W. E. A. DAVIES, *J. Phys. D* **7** (1974) 120.
12. T. JOY and W. STREIDER, *J. Phys. C* **11** (1978) L867.
13. *Idem, J. Comp. Mater.* **13** (1979) 102.
14. *Idem, J. Phys. C* **12** (1979) L279.
15. J. E. SCHOUTENS and F. S. ROIG, *J. Mater. Sci.* in press.
16. K. R. KARASEK and J. BEVK, *J. Appl. Phys.* **52** (1981) 1370.
17. R. SIMONEAU and G. BEGIN, *ibid.* **45** (1974) 3828.
18. *Idem, ibid.* **44** (1973) 1461.
19. B. N. ALEKSANDROV and I. G. D'YAKOV, *Soviet Phys. JETP* **16** (1963) 603.
20. B. N. ALEKSANDROV, *ibid.* **16** (1963) 286.
21. B. N. ALEKSANDROV and M. I. KAZANOV, *ibid.* **14** (1962) 948.
22. F. S. ROIG and J. E. SCHOUTENS, unpublished data, 1905.
23. F. S. ROIG and J. E. SCHOUTENS, "The Electrical Conductivity of Thin-wall Tubes", unpublished data, 1984.
24. *Idem, J. Mater. Sci.* **21** (1986) 2767.
25. J. M. ZIMAN, "Electrons and Phonons" (Oxford University Press, Oxford, U.K. 1960) Ch. 7.
26. C. R. CHESTER, "Techniques in Partial Differential Equations" (McGraw-Hill, New York, 1971) Ch. 8.
27. D. L. LESSIE and E. R. CROSSON, *J. Appl. Phys.* **59** (1986) 504.
28. I. S. GRADSHTEYN and I. M. RYZHIK, "Tables of Integrals, Series, and Products" (Academic, New York, 1965) p. 49.
29. F. S. ROIG and J. E. SCHOUTENS, *J. Mater. Sci.* in press.

Received 12 January and accepted 1 April 1987